

CHAPTER 179

SUSPENDED SEDIMENT CAUSED BY WAVES AND CURRENTS

Masanobu Ono¹⁾, Kyu Han Kim²⁾, Toru Sawaragi³⁾ and
Ichiro Deguchi⁴⁾

Abstract

A procedure to estimate vertical diffusion coefficient and reference concentration of time averaged suspended sediment concentration caused by waves and current are discussed based on experimental results obtained in a laboratory.

It is found that the non-dimensional diffusion coefficient normalized by the product of shear velocity u^* and the equivalent roughness k_s , is more closely related to the Shields' number when the shear velocity is evaluated by using the equivalent roughness where the effect of ripple geometry is taken into account. The reference concentration is not a unique function of the sediment Shields' number. Incident wave period has also influence on the reference concentration.

Introduction

Waves and currents around coastal structures and navigation channels have large spatial gradients that cause non-equilibrium sediment transport. In the analysis of topographic changes around these obstacles, we have to take into account the effect of non-equilibrium property of sediment transport. Especially, non-equilibrium property of suspended sediment rather than that of bed load plays very important role. Because it takes bed particles a little time to adopt themselves to the new surroundings and there is an instantaneous adjustment to equilibrium state in the very vicinity of the bottom.

To evaluate suspended sediment transport rate based on an advection-diffusion equation, we have to know both concentration and transporting velocity. The authors have already developed highly accurate numerical procedure for solving the advection-diffusion equation by applying a split-operator approach (Komatsu, et al., 1985). The accuracy of the numerical procedure deeply depends on a boundary

¹⁾Research Assoc., ³⁾Prof., and ⁴⁾Assoc. Prof., Dept. of Civil Engineering, Osaka University, Yamada-oka, Suita-city, Osaka 565, Japan

²⁾Assis. Prof., Dept. of Civil Engineering, Kwan-Dong University, Korea

condition at the bottom (reference concentration or vertical sediment flux at the bottom) and diffusion coefficient. Until now, many studies have been conducted about suspended sediment due to waves in equilibrium state. Only a few have been carried out about the non-equilibrium suspended sediment concentration and the effect of current superposed on waves.

The aim of this study is to investigate the effect of current on suspended sediment, especially the reference concentration and the vertical diffusion coefficient of suspended sediment, through experiments.

Typical example of topographic change caused by non-equilibrium sediment transport

First of all, we briefly examine the characteristics of non-equilibrium suspended sediment concentration measured in an experiment and an applicability of the numerical procedure for predicting non-equilibrium sediment concentration. Figure 1 shows the typical example of non-equilibrium suspended sediment transport caused by waves and current.

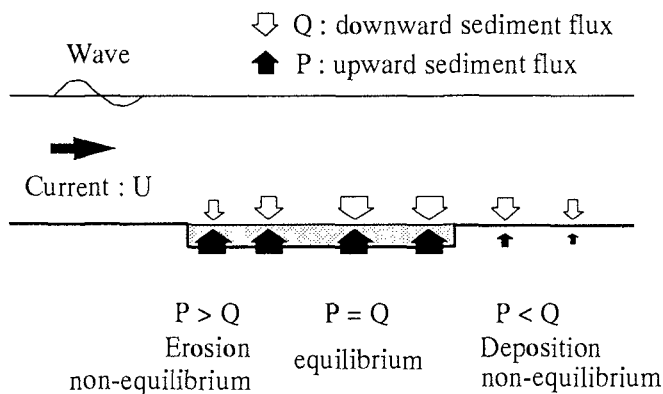


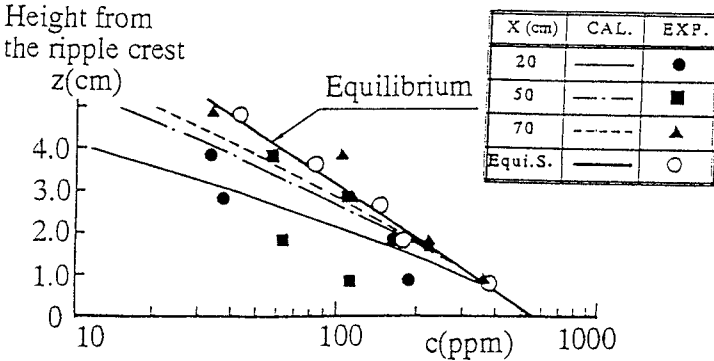
Fig. 1 Typical example of non-equilibrium suspended sediment transport

The waves and current are in the same direction on a horizontal bottom where a part of the bottom was replaced by a movable bed. Around the both sides of the movable bed, non-equilibrium suspended sediment transport takes place due to the unbalance of upward and downward sediment flux. Near the upstream end of the movable bed, only upward transport occurs and there is little settling flux and water depth increases. Near the downstream end of the movable bed, there is no upward sediment flux and only settling flux exists. It is needless to say that the water depth decreases there.

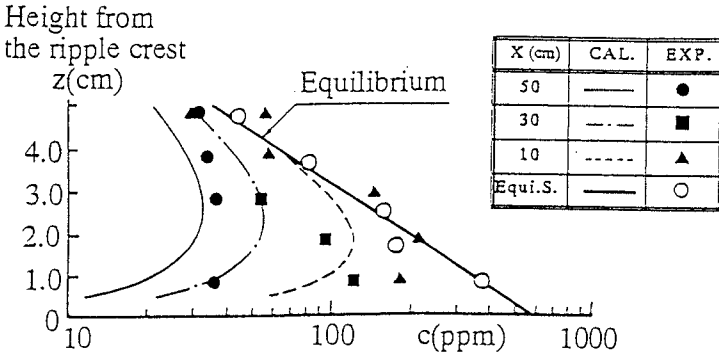
To predict non-equilibrium suspended sediment concentration numerically, the details of which I will mention later, we have to give reference concentration and diffusion coefficient. We should fundamentally use reference concentration and diffusion coefficient for suspended sediment under the non-equilibrium condition.

However, there are various degree of non-equilibrium property and it is difficult to obtain universal expression of reference concentration and diffusion coefficient under the non-equilibrium condition. Then we tentatively use those values obtained from the experiment under the equilibrium condition.

Figure 2 shows the comparisons of measured and calculated distribution of suspended sediment concentration. Fig.(a) is the non-equilibrium state near the upstream end of the movable bed. Fig.(b) is the results near the downstream end of the movable bed. x axis is taken positive in the direction of waves and currents from the edge of upward movable bed.



(a) Distribution of non-equilibrium sediment concentration near the upstream end of the movable bed



(b) Distribution of non-equilibrium sediment concentration near the downstream end of the movable bed.

Fig. 2 The comparisons of the numerical results and measured value of the vertical distribution of non-equilibrium suspended sediment concentration. ($h=20\text{cm}$, $D=0.012\text{cm}$, $U=17\text{cm/sec}$, $T=1.25\text{sec}$, $H=6\text{cm}$)

In spite of the usage of reference concentration and diffusion coefficient of equilibrium condition, the numerical results coincide with the measured results relatively well. So we can judge that we can predict non-equilibrium suspended

sediment concentration by applying the split operator approach provided that we can give the reference concentration and diffusion coefficient even under the equilibrium state.

Experiments for diffusion coefficient and reference concentration of equilibrium suspended sediment concentration

Experiments were carried out in two two-dimensional wave tanks of different size. Length, depth and width of a large tank were 30m*1.9m*1.8m and those of a small tank were 30m*0.9m*0.7m. Two kinds of bed materials of mean diameter $D=0.012\text{cm}$ and 0.035cm were used to make a movable bottom of the length 3m (in a small tank) and 6m (in a large tank). All experiments were conducted on a horizontal bottom of water depth between 10cm to 40cm. The range of wave height was 5cm to 20cm and wave period was 1second to 2.5seconds. In the small tank experiments, we generated current in the direction of wave propagation. The relative magnitude of current and wave U/u_b varied from 0 to 0.9, where U is the depth averaged velocity of current and u_b is the water particle velocity at the bottom due to waves. Some parts of the experiments were conducted by generating irregular waves of Bretschneider-Mitsuyasu type frequency spectrum.

Suspended sediment concentration was measured by using an optical sensor and sampling of sediment laden water. Figure 3 shows an examples of vertical distributions of time averaged suspended sediment concentration measured at the crest and the trough of the ripple.

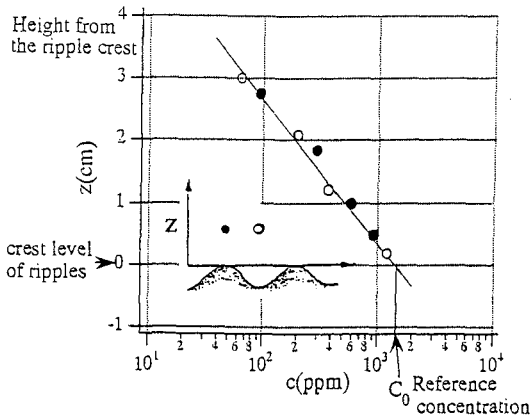


Fig. 3 Examples of vertical distributions of time averaged suspended sediment concentration measured at the crest and the trough of the ripple. ($h=20\text{cm}$, $D=0.012\text{cm}$, $T=1.5\text{sec}$, $H=6\text{cm}$)

As has already been pointed out by many researchers, there is not any significant difference between the vertical distribution of time averaged concentration

measured on the crest and that measured at the trough and the time averaged concentration of suspended sediment became a log-linear vertical distribution. This implies that the diffusion coefficient of suspended sediment κ_z becomes constant through the depth.

In the figure, our methods to determine diffusion coefficient and reference concentration from experimental results are also illustrated. We evaluated diffusion coefficient from the vertical distribution of suspended sediment concentration and the relation shown by Eq.(1) that is derived from the usual one-dimensional diffusion equation in a steady state.

$$\kappa_z = -\frac{w_f z}{\log(c/C_0)} \quad (1)$$

where κ_z is the diffusion coefficient, w_f is the settling velocity.

The value of reference concentration C_0 was determined from concentration at the crest level of ripples.

In the analyses of the diffusion coefficient and reference concentration, the experimental results obtained by other researchers that have already been published in journals and proceedings are also used together with our experimental results.

Estimation of bottom shear stress and shear velocity under wave-current coexisting field

The diffusion coefficient and reference concentration are deeply related to a bottom shear stress or friction velocity under wave-current coexisting field. Equation (2) is our expression of the bottom shear stress $\tau_{cw}(t)$ due to waves and current derived by solving a turbulent boundary layer equation (Deguchi, 1995) where the maximum shear velocity u_{cw}^* is given by Eq.(3).

$$\begin{aligned} \tau_{cw}(t) &= \tau_c + \tau_w(t) \\ &= \rho u_c^{*2} + \rho \hat{u}_{bp} \sqrt{\kappa \sigma z_0 u_{cw}^*} (R_{wp}^{\prime 2} + I_{wp}^{\prime 2})^{1/2} \cos(\sigma t - \psi') \quad (2) \\ \psi' &= \tan^{-1}(I_{wp}' / R_{wp}') \end{aligned}$$

$$\frac{u_{cw}^*}{u_b} = \frac{u_c^*}{u_b} + \sqrt{\kappa \left(\frac{z_0}{a_b} \right) \left(\frac{u_{cw}^*}{u_b} \right) (R_{wp}^{\prime 2} + I_{wp}^{\prime 2})^{1/2}} \quad (3)$$

$$R_{wp}' = 1 - \frac{\ker' q_0 \ker q_0 + \kei' q_0 \kei q_0}{(\ker q_0)^2 + (\kei q_0)^2}, \quad I_{wp}' = \frac{\ker' q_0 \kei q_0 + \kei' q_0 \ker q_0}{(\ker q_0)^2 + (\kei q_0)^2}$$

where $q_0 = 2\{z_0 / (\kappa u_{cw}^* / \sigma)\}^{1/2}$, u_c^* is the bottom shear velocity due to current, z_0 is the height of roughness element, σ is the angular frequency, κ is the Karman's constant and \ker and \kei are the real and the imaginary parts of the modified Bessel Functions of 2nd. kind, \ker' and \kei' are the derivatives of \ker and \kei , respectively.

The depth-averaged velocity U is calculated by integrating the steady velocity between $z=z_0$ and h . From this relation, the bottom shear velocity u_c^* with respect to the mean current is expressed by Eq.(4)

$$\frac{u_c^*}{u_b} = \frac{1}{2} \left\{ -\left(\frac{\alpha_2}{\alpha_1}\right)\left(\frac{u_{cw}^*}{u_b}\right) + \sqrt{\left(\frac{\alpha_2}{\alpha_1}\right)^2\left(\frac{u_{cw}^*}{u_b}\right)^2 + 4\kappa\left(\frac{U}{u_b}\right)\left(\frac{u_{cw}^*}{u_b}\right)\frac{h-z_0}{\alpha_1}} \right\} \quad (4)$$

$$\alpha_1 = h \ln(\delta_w/z_0) - \delta_w + z_0 \quad \alpha_2 = h \ln(h/\delta_w) - h + \delta_w$$

where δ_w is the thickness of wave boundary layer.

Figure 4 illustrates the comparison of measured and calculated distribution of mean current. Solid line is the calculated vertical distribution of mean current velocity without waves and the broken line is the calculated velocity profile in the case of wave and current coexisting field. Open and closed circles in the figure are the time averaged measured velocity in the cases of no waves and wave-current coexisting field.

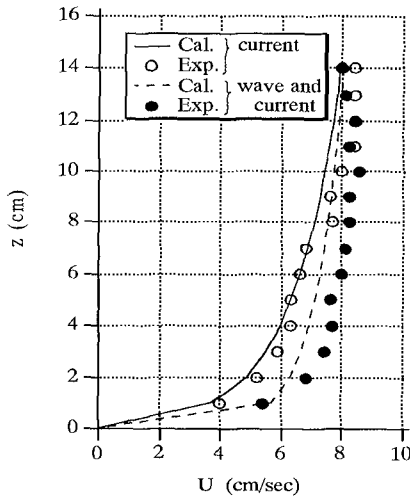


Fig. 4 Vertical distribution of mean current velocity in the case of wave and current coexisting field. ($h=20\text{cm}$, $D=0.012\text{cm}$, current, $U=7.0\text{cm/sec}$; wave and current : $T=1.5\text{sec}$, $H=6\text{cm}$, $U=7.5\text{cm/sec}$)

The velocity was measured by an electromagnetic current meter. It is found that the calculated velocity profile reproduce the measured profile. It is also found that the presence of waves increases the kinematic eddy viscosity that results in the steep velocity profile.

Results and discussion

(1) Diffusion coefficient

Here we examine the expression of diffusion coefficient based on the continuity equation of suspended sediment concentration that is expressed by Eq.(5).

$$\frac{\partial c}{\partial t} + \frac{\partial}{\partial x}(cu_s) + \frac{\partial}{\partial z}(cw_s) = 0 \quad (5)$$

We decompose the variables in Eq.(5) into steady part, wave and turbulent components and express each component by using an over bar(-), subscript p and (') as follows:

$$c = \bar{c} + c_p + c'$$

$$u_s = \bar{u}_s + u_{sp} + u_s' \quad (6)$$

$$w_s = -\bar{w}_f + w_{sp} + w_s'$$

Substituting these components into Eq.(5) and taking time average, we obtain Eq.(7)

$$\frac{\partial \bar{c}}{\partial t} + \frac{\partial}{\partial x}(\overline{cu_s}) - \frac{\partial}{\partial z}(\overline{cw_s}) = \frac{\partial}{\partial x} \left(\kappa_x \frac{\partial \bar{c}}{\partial x} \right) + \frac{\partial}{\partial z} \left(\kappa_z \frac{\partial \bar{c}}{\partial z} \right) \quad (7)$$

where the diffusion coefficient is expressed by Eqs.(8) and (9).

$$\kappa_x = -(\overline{c_p u_{sp}} + \overline{c' u_s'}) / \frac{\partial \bar{c}}{\partial x} \quad (8)$$

$$\kappa_z = -(\overline{c_p w_{sp}} + \overline{c' w_s'}) / \frac{\partial \bar{c}}{\partial z} \quad (9)$$

The first term of Eq.(7) is neglected in a steady state. We assume here that horizontal gradient of mean current velocity is negligibly small and all variables are uniform in x-direction. Then Eq.(5) becomes a usual one dimensional diffusion equation.

On the other hand, Schmidt number is usually defined as Eq.(10)

$$\text{Schmidt number} = \varepsilon_z / \kappa_z \quad (10)$$

where ε_z is the kinematic eddy viscosity. It is often assumed that the order of Schmidt number is unity. If we adopt this assumption, the diffusion coefficient can be expressed in the same way as the kinematic eddy viscosity. We used the following form of the kinematic eddy viscosity as shown in Eq.(11) to solve the boundary layer equation:

$$\varepsilon_z \approx \kappa u_{cw}^* l \quad (11)$$

where l is the length scale.

According to this expression, we assume that the velocity scale and length scales of the diffusion coefficient be the shear velocity u^* and equivalent roughness k_s . The value of u^* depends on the expression of k_s . In the following, we will examine the relation between non-dimensional diffusion coefficient and Shields' number calculated by using two different expression of k_s , Eq.(12) and (13). Eq. (13) is proposed by Nielsen(1992) includes the effect of ripple geometry.

$$l = k_s = 2.5D \quad (12)$$

or

$$k_s = 8\eta^2 / \lambda + 5\phi_D D \quad (13)$$

Fig.5 is the result obtained by using Eq.(12) where we assume that the value of k_s is a unique function of D .

The vertical axis is the diffusion coefficient normalized by dividing measured diffusion coefficient by the product of u^* and k_s . The horizontal axis is grain roughness Shields' number ϕ_D defined by Eq.(14).

$$\phi_D = u^{*2} / (\sigma' gD) \tag{14}$$

where u^{*1} is the shear velocity calculated by using Eq.(12), σ' is the immersed grain density, g is the gravity acceleration. In this case plotted data scatters in a wide range.

Author	Symbol	U/u_b	$\alpha=D/(f_w T)$	wD/v
Present study	I.W.	●	0	0.37-1.40
Present study	R.W.	○	0	0.22-0.31
Nielsen(1986)	R.W.	+	?	0.44
Staub et al.(1984)	O.F.	×	0	0.12-0.16
Tanaka et al.(1973)	R.W.C.	□	0	0.25-0.32
		▤	0.1- 0.5	0.21-0.30
		▥	0.5- 0.9	0.17-0.24
		▦	-0.1- -0.5	0.23-0.30
		▧	-0.5- -0.9	0.16-0.20
Present study	R.W.C.	△	0	0.16-0.19
		▲	0.2-0.4	0.15-0.18
		▴	0.4-0.7	0.13-0.17
		▵	0.7-0.9	0.11-0.15
Nakato et al.(1977)	O.F.	◇	0	0.27-0.47
Hayakawa et al.(1983)	O.F.	◇	0	0.15-0.19
Nielsen(1984)	F	◆	?	0.07-0.19

I.W.: Irregular waves, R.W.: Regular waves, O.F.: Oscillatory flow,
R.W.C.: Regular waves and currents, F: Field

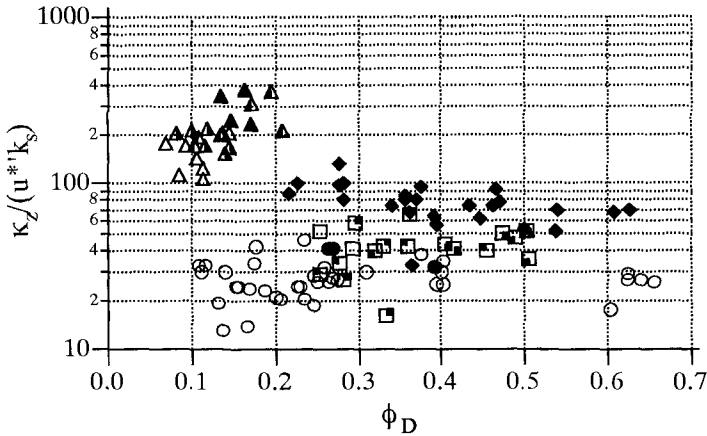


Fig. 5 Relation between non-dimensional diffusion coefficient and grain roughness Shields' number

Fig.6 shows the relation between non-dimensional diffusion coefficient and ripple roughness Shields' number ϕ_η .

The vertical axis is again the non-dimensional diffusion coefficient and the horizontal axis is the ripple roughness Shields' number ϕ_η defined by Eq.(15).

$$\phi_\eta = u^{*2} / (\sigma' gD) \tag{15}$$

where u^* is the shear velocity calculated by using Eq.(13).

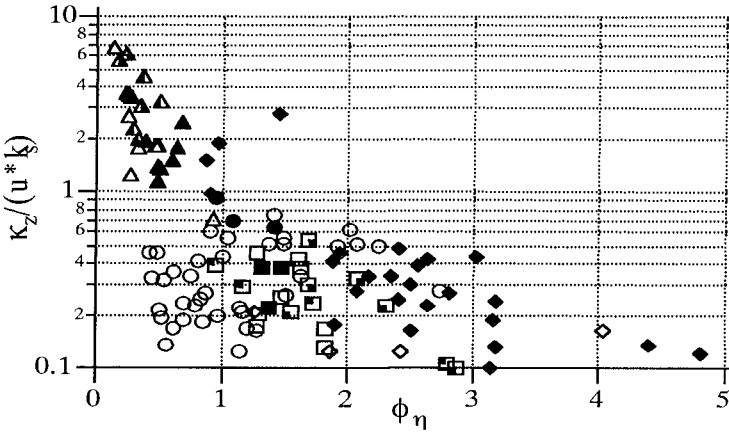


Fig. 6 Relation between non-dimensional diffusion coefficient and ripple roughness Shields' number

In this case, the scattering of data becomes small when compared with the data shown in Fig.(5). This implies that the length scale of the diffusion coefficient depends on vortex formation around ripples.

In the figure, the results obtained in the irregular wave experiments are also shown. The bottom shear velocity is calculated by using wave characteristics with respect to the rms wave height.

It was reported that there were no regular ripples on the bottom and sheet flow transport just begun in the case where ripple roughness Shields' number is greater than three. When ϕ_η is larger than 0.7, the non-dimensional diffusion coefficient varies from 0.1 to 0.6. In the region where ϕ_η is smaller than 0.7, non-dimensional diffusion coefficient increases a little with the increases in the value of U/u_b . In this region, waves have not large power to bring sediment into suspension and contribution of current to suspension becomes relatively large. However, it required further investigation about turbulence generated by ripples and diffusibility of suspended sediment to quantitatively estimate the value of diffusion coefficient.

(2)Reference concentration

We have already proposed semi-empirical expression for predicting reference concentration based on energetic consideration. The outline of the derivation of the expression for reference concentration are shown below.

We assumed that a part of the turbulent energy of vortex generated in the ripple trough is used to bring sediment into suspension. Tunstall and Inmen (1975) evaluated the kinematic energy of vortex formed in the trough of ripples that is expressed by Eq.(16) (see Fig. 7)

$$Ev = 2.26\rho(\Gamma/2\pi)^2 \tag{16}$$

where Γ is the strength of vortex circulation and is given by Eq.(17).

$$\Gamma / 2\pi = 0.39u_b\eta \tag{17}$$

The work W_v that is required to keep suspended sediment of the concentration C_0 in the vortex whose diameter r_v is estimated by Eq.(18)

$$W_v = \rho C_0 \sigma' g w_f (T/2) r_v^2 \tag{18}$$

where r_v is expressed by the relation of Eq.(19).

$$r_v = 0.6\eta \tag{19}$$

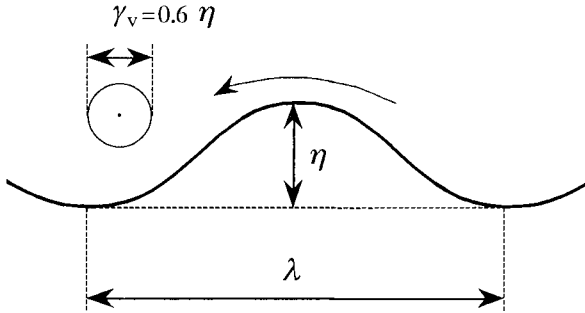


Fig. 7 Vortex generated on the ripple

We further assume that a part of E_v is used to keep sediment into suspension.

$$W_v \propto E_v \tag{20}$$

This leads to the following expression for C_0 .

$$C_0 = \beta u_b^2 / (\sigma' g w_f T) \tag{21}$$

where β is the empirical coefficient.

When we replace u_b by using a shear velocity, we can finally obtain the expression of the reference concentration

$$C_0 = 0.49(\alpha \phi_D)^{1.77} \tag{22}$$

$$\alpha = D / (f_w w_f T)$$

where f_w is Jonsson's friction factor and T is wave period.

Figure 8 shows the relation between measured reference concentration C_0 and grain roughness Shields' parameter ϕ_D .

Straight lines in Fig.8 are the reference concentrations calculated from Eq.(22) for the various values of α . In the figure, expression of reference concentration proposed by Fredsøe et al.(1978) is also shown. Measured reference concentration increases with the increase of the value of α as was predicted by Eq.(22).

Measured reference concentration caused by wave and current decreases with the increase in the value of U/u_b . A ripple geometry was deformed into asymmetry by the presence of current. Significant suspended sediment cloud was generated only once within one wave period from the steep side of the ripple. Consequently, time

averaged concentration at the bottom (reference concentration) decreases when current exists.

To figure out the reference concentration in the presence of current, further investigation is required about asymmetrical property of generated ripples and flow field on them.

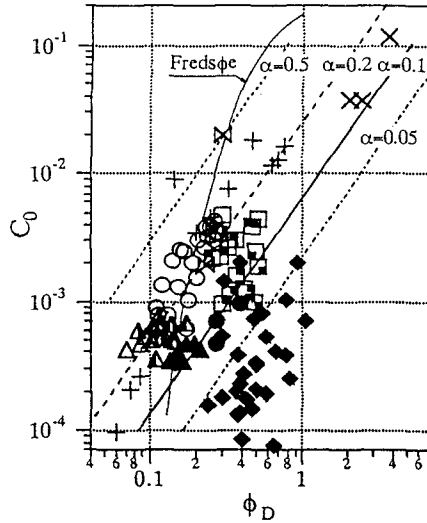


Fig. 8. Relation between measured reference concentration C_0 and grain roughness Shields' parameter ϕ_D .

Conclusions

Characteristics of the vertical diffusion coefficient and the reference concentration of time averaged suspended sediment concentration caused by waves and current are examined based on the experimental results obtained in laboratory.

It is found that the non-dimensional diffusion coefficient normalized by the product of the shear velocity and the roughness element is closely related to the ripple roughness Shields' number when the shear velocity is evaluated using the relative roughness that includes the effect of ripple geometry. When ripple roughness Shields' number is larger than 3, ripples lose their two-dimensional shape and the non-dimensional diffusion coefficient becomes small.

Current superimposed on waves deforms ripple shape into asymmetry and the reference concentration of suspended sediment caused by waves and current decreases with the increase in the relative magnitude of current U/wb . The reference concentration is not a unique function of the sediment Shields number and incident wave period also influence the reference concentration as was expected from the energetic consideration shown in the paper.

Reference

Deguchi, I., 1995, Waves, wave-induced currents and sediment transport, in "Coastal Engineering-Waves Beaches and Wave-Structure Interactions-", Edited by. T. Sawaragi, Elsevier Science B.V. (in printing).

Fredsoe, J., O.H. Andersen and S. Siberg, 1978, Distribution of suspended sediment in large waves, Proc. ASCE, Vol.110, No.ww2, pp.215-230.

Hayakawa, N., G. Tsujimoto and H. Hashimoto, 1983, Velocity distribution and suspended sediment concentration over large scale ripple, Coastal Eng. in Japan, Vol.26, pp.91-100.

Komatsu, T., F.M. Holly, Jr., N. Nakashiki and K. Ohguchi, 1985, Numerical calculation of pollutant transport in one and two dimensionals, JHHE, Vol.3, No.2, pp.15-30.

Nakato, T., F.A. Locher, J.G. Glove and J.F. Kennedy, 1977, Wave entertainment of sediment from rippled bed, Proc. ASCE, Vol.103, No.ww1, pp.83-99.

Nielsen, P., 1984, Field measurements of time averaged suspended sediment concentrations under waves, Coastal Engineering, Vol.8, pp.21-72.

Nielsen, P., 1986, Suspended sediment concentrations under waves, Coastal Engineering, Vol.10, pp.23-31.

Nielsen, P., 1992, Coastal bottom boundary layers and sediment transport, Advanced Series on Ocean Engineering, Vol.4, 324p.

Sawaragi, T., I. Deguchi, M. Ono and K.S. Bae (1991), Numerical simulation for shoaling process of navigation channel, Int'l. Sympo. on Natural Disaster Reduction and Civil Engineering, JSCE, pp.117-126.

Tanaka, N., H. Ozawa and A. Ogasawara, 1973, Experiments on sand movement by waves and currents, Rept. Port and Harbour Res. Inst., Vol.12, No.4, pp.2-22 (in Japanese).

Tunstall, E.B. and D.L. Inman, 1975, Vortex generation by oscillatory flow over rippled surface, J.G.R., Vol.80, No.24, pp.3475-3484.